Representations with poles and cuts for the time-domain simulation of fractional systems and irrational transfer functions

Thomas Hélie

Laboratoire des Sciences et Technologie de la Musique et du Son, Equipe Analyse/Synthèse. CNRS UMR 9912 - Ircam, Centre Georges Pompidou. 1, place Igor Stravinsky. 75004 Paris, France.

Denis Matignon *

Laboratoire Traitement et Communication de l'Information, Département Traitement du Signal et des Images. CNRS UMR 5141 - Télécom Paris. 37-39, rue Dareau 75014 Paris, France.

Abstract

Fractional differential systems are infinite-dimensional systems which are difficult to study and simulate: they can be represented with *poles and cuts*. This representation applies to a wider class of irrational transfer functions, and is most useful for signal processing purposes, such as frequency-domain and time-domain simulations: the approximations in low dimension which give the most striking numerical results are obtained through an optimization procedure, the parameters of which are meaningful from a signal point of view. Ten such systems of increasing complexity are thoroughly investigated.

Key words: infinite dimensional systems, irrational transfer functions, time-domain simulation, fractional differential systems, diffusive representations
PACS: 02.30.Gp., 02.60.Cb., 02.60.Pn.

* Correponding author
Email addresses: Thomas.Helie@ircam.fr (Thomas Hélie), matignon@tsi.enst.fr (Denis Matignon).
URL: http://www.tsi.enst.fr/∼matignon (Denis Matignon).

1 Introduction

There are many linear systems with irrational transfer functions, especially transfer functions of mathematical physics which involve *fractional* powers of the Laplace variable s. A wide class of such special functions can be found in e.g. [12], and some of them are given infinite-dimensional representations as in [9]. A more specialized literature concentrates on fractional differential systems, such as [15], [11] for physical models, [7] for the mathematical theory, and [10] for an interplay between signal processing, control theory and applications of such systems and their generalization.

The question of representing these systems in a somewhat closed form, or in a way which is more suitable for computation, not only in the frequency but also the time domain, is seldom asked and rarely answered in a satisfactory way. The aim of this paper is to give some answers to these questions, with a point of view which lies half way between signal processing and control theory: for short, complicated case studies will be introduced, analysed and simulated thoroughly.

2 Examples of systems involving fractional derivatives

We select a family of ten linear systems, which involve either fractional derivatives in the time domain, or fractional powers of the Laplace variable s in their transfer function. Most of them stem from a physical example, which can be very simple or quite involved, but this is not the point at stake in the present paper: we are more interested here in presenting a kind of a hierarchy of *fractional* systems.

2.1 An introductory example

The following transfer function is irrational, but can be simply represented by a series of first-order systems:

$$H_1(s) = \frac{\tanh(\sqrt{s})}{\sqrt{s}} = \sum_{n \in \mathbb{N}} \frac{2}{s + (n + \frac{1}{2})^2 \pi^2}. \tag{1}$$

Note that there are other examples of the same kind, which involve hyperbolic trigonometric functions and $\sqrt{s}$, for which a series expression is available, see e.g. [9].

The classical integral or derivative operators of fractional order also have irrational transfer functions, which cannot be represented by a series of first-order systems, but can be exactly represented by a *continuous* superposition of first-order systems (sometimes called diffusive representation) with some weight μ, which can be computed analytically:

$$H_2(s) = \frac{1}{s^\beta} \qquad 0 < \Re e(\beta) < 1, \tag{2}$$

$$H_3(s) = s^\alpha \qquad 0 < \Re e(\alpha) < 1. \tag{3}$$

In the sequel, the output of system $H_3(s) = s\,\frac{1}{s^{1-\alpha}}$ will be considered as the (integer) time-derivative of the output of system H_2 with parameter $\beta = 1-\alpha$; this simple remark will apply both for equivalent representations and simulation purposes. A technical well-posenedness condition on this weight μ will distinguish between the two cases H_2 and H_3. This condition of theoretical nature will also have numerical implications.

2.3 Fractional differential systems

A more complex combination of fractional derivatives gives rise to the so-called fractional differential systems, the transfer function of which reads:

$$\text{either } H_4(s) = R(s^\alpha) = \frac{Q(s^\alpha)}{P(s^\alpha)} = \frac{\sum_{l=0}^{l=q} b_l\, s^{l\,\alpha}}{\sum_{k=0}^{k=p} a_k\, s^{k\,\alpha}} \qquad 0 < \Re e(\alpha) < 1, \tag{4}$$

$$\text{or } H_5(s) = \frac{\sum_{l=0}^{l=q} b_l\, s^{\beta_l}}{\sum_{k=0}^{k=p} a_k\, s^{\alpha_k}} \qquad \left| \begin{array}{l} 0 < \Re e(\beta_l) < \Re e(\beta_{l+1}), \\ 0 < \Re e(\alpha_k) < \Re e(\alpha_{k+1}). \end{array} \right. \tag{5}$$

The first case H_4 is known as fractional differential systems of *commensurate* order α, wich allows the use of some algebraic tools for equivalent representation, stability analysis and also simulation purposes.

On the contrary, the more general case H_5 is known as fractional differential systems of *un*commensurate orders: for these systems, no algebraic tools can be applied, and both their analysis and simulation are quite involved.

Many results are known for these systems, as will be recalled later in § 3.2.3.

2.4 Diffusive systems

Let us now consider examples which are neither a series of first-order systems, nor fractional differential systems, such as:

$$H_6(s) = \frac{e^{-\sqrt{s}}}{\sqrt{s}}, \tag{6}$$

$$H_7(s) = e^{-\sqrt{s}}. \tag{7}$$

Both can be decomposed on a *continuous* family of first-order systems with negative real poles $-\xi$, with a specific weight $\mu(\xi)$ playing exactly the same role as residues at the poles $s = -\xi$. The technical well-posenedness condition on the weight μ will distinguish between the two cases H_6 and H_7; exactly for the same reason, a distinction was made between H_2 and H_3 earlier in § 2.2.

2.5 More complex systems

Let us now consider some strange systems, the transfer function of which have poles of finite order and branching points with cuts to be chosen between them:

$$H_8(s) = \frac{1}{\sqrt{s^2+1}} \tag{8}$$

is the transfer function of the causal Bessel function of order zero $J_0(t)$, and it has been studied first in [3, § 3.3], then in [19], and finally in [8, Example 3.1] with a new integral representation, which shows much freedom in the choice of the cuts between the two fixed branching points, namely $s = \pm i$.

Now, some more intricate transfer functions can easily be met on more complex examples,

$$H_9(s) = e^{s-\Gamma(s)}, \qquad \text{with } \Gamma(s) = \sqrt{s^2 + \varepsilon\, s^{\frac{3}{2}} + 1}, \quad \text{and } \varepsilon > 0 \tag{9}$$

$$H_{10}(s) = \frac{2\Gamma(s)}{s+\Gamma(s)}\, e^{s-\Gamma(s)}\,. \tag{10}$$

They are involved in the description of a 1-D wave equation in a flared duct of finite length, with viscothermal losses at the boundary: see e.g.[17] for a

theoretical study of this model, [18,16] for simulation of these transfer functions, and [20, chapter 9] for a study of the modal decomposition related to this model.

3 Integral representations with poles and cuts

We now investigate the general integral representations in the complex plane with poles and cuts: we present the general framework, and then apply it to the ten examples presented in section 2.

3.1 General framework

Many transfer functions can be decomposed as follows, in some right-half complex plane $\Re e(s) > a$,

$$H(s) = \sum_{k=1}^{K} \sum_{l=1}^{L_k} \frac{r_{k,l}}{(s-s_k)^l} + \int_{\mathcal{C}} \frac{M(\mathrm{d}\gamma)}{s-\gamma}\,, \tag{11}$$

which translates in the time domain into the following decomposition of the impulse response:

$$h(t) = \sum_{k=1}^{K} \sum_{l=1}^{L_k} r_{k,l} \frac{1}{l!} t^{l-1}\, e^{s_k\, t} + \int_{\mathcal{C}} e^{\gamma\, t}\, M(\mathrm{d}\gamma), \qquad \text{for } t > 0. \tag{12}$$

The time-domain simulation of the *finite-dimensional part* of size $\sum_{k=1}^{K} L_k$ is really standard and will not be detailed in the sequel. The time-domain simulation of the *infinite-dimensional part* of these systems can quite easily be done through the following continuous family of *first-order differential systems*, parametrized by $\gamma \in \mathcal{C}$:

$$\partial_t \phi(\gamma, t) = \gamma\, \phi(\gamma, t) + u(t), \quad \phi(\gamma, 0) = 0, \qquad \forall \gamma \in \mathcal{C} \tag{13}$$

$$y(t) = \int_{\mathcal{C}} \phi(\gamma, t)\, M(\mathrm{d}\gamma)\,, \tag{14}$$

which is nothing but an input u-state ϕ-output y representation of our system.

In all the integral equations above, $\mathcal{C}$ is a contour in some left-half complex plane, and M is a *measure* on this contour. Once a parametrization has been chosen for the contour, the measure can be decomposed into different parts,

such as a purely discrete part (Dirac measures at some points in some left-half *complex* plane) and an absolutely continuous part $\mu(\gamma)$ with respect to the Lebegue measure $\mathrm{d}\gamma$. A straightforward interpretation can therefore be proposed: $\mu(\gamma)$ plays the role of the residue at the pole $s = \gamma$.

But of course, these representations make sense only if a so-called *well-posedness condition* is fulfilled, namely:

$$\int_{\mathcal{C}} \left| \frac{M(\mathrm{d}\gamma)}{a+1-\gamma} \right| < \infty \,. \tag{15}$$

We refer to [5, § 5 and § 6] for the general theory and [4] for the implications of the well-posedness condition.

When M has a density, an analytical computation of μ can be performed from H accross the cut, taking non-tangential limits; when $\mathcal{C} = \mathbb{R}^-$, we find with e.g. [3]:

$$\mu(\xi) = \lim_{\varepsilon \to 0^+} \frac{1}{2i\pi} \left\{ H(-\xi - i\varepsilon) - H(-\xi + i\varepsilon) \right\} , \tag{16}$$

a formula which will be most useful in the sequel, namely in § 3.2.

As already mentioned in section 2, in some cases, since the well-posedness condition (15) is not met, an extension can be proposed, which is still meaningful in some larger mathematical framework, namely:

$$\breve{H}(s) = s \int_{\mathcal{C}} \frac{M(\mathrm{d}\gamma)}{s-\gamma} + \breve{H}(0) \,, \tag{17}$$

which gives rise to the following input u-state ϕ-output z representation in the time domain:

$$\partial_t \phi(\gamma, t) = \gamma\, \phi(\gamma, t) + u(t), \quad \phi(\gamma, 0) = 0, \qquad \forall \gamma \in \mathcal{C} \tag{18}$$

$$z(t) = \int_{\mathcal{C}} \partial_t \phi(\gamma, t)\, M(\mathrm{d}\gamma) + \breve{H}(0)\, u(t) \,. \tag{19}$$

Let us now go back to our examples and see how they fit in the general framework.

3.2.1 An introductory example

Choosing $\mathcal{C} = \mathbb{R}^-$ leads to $M_1 = \sum_{n\in\mathbb{N}} 2\,\delta(\xi - (n+\frac{1}{2})^2\pi^2)$ with $\gamma = -\xi$, and (15) is fulfilled.

3.2.2 Fractional integrals and derivatives

Choosing $\mathcal{C} = \mathbb{R}^-$ and $\gamma = -\xi$ leads to $\mu_2(\xi) = \frac{\sin(\beta\pi)}{\pi}\frac{1}{\xi^\beta}$, which fulfills (15).

But H_3 must be realized with an extension: $H_3(0) = 0$ and $\breve{\mu}_3 = \mu_2$ with the particular choice $\beta = 1-\alpha$; thus, $\breve{\mu}_3$ now fulfills (15).

3.2.3 Fractional differential systems

3.2.3.1 Commensurate orders Following e.g. [2, § 2.2], one can decompose the impulse response of system H_4 into a finite sum of special functions, namely *Mittag-Leffler* functions (defined by $\mathcal{E}_\alpha(\lambda,t) = t_+^{\alpha-1}\sum_{k=0}^{\infty}\frac{(\lambda t_+^\alpha)^k}{\Gamma((k+1)\alpha)}$ when the roots of P in (4) are simple, see [21]). Hence, the transfer function reads $H_4(s) = \sum_{n=1}^{p} r_n\,(s^\alpha - \lambda_n)^{-1}$, and the impulse response reads:

$$h_4(t) = \sum_{n=1}^{p} r_n\,\mathcal{E}_\alpha(\lambda_n, t)\,. \tag{20}$$

This decomposition looks finite dimensional, but the following remarks apply:

- from a numerical point of view, these special functions are difficult to compute in the *whole* complex plane (since $\lambda_n \in \mathbb{C}$); even in the case $\alpha = \frac{1}{2}$, where the function is easily related to the classical *error function*, the argument is not limited to $\mathbb{R}$, and this makes the problem difficult;
- this decomposition allows an *algebraic* knowledge of the poles and residues (namely $s_n = (\lambda_n)^{\frac{1}{\alpha}}$ and $r_n = \frac{1}{\alpha}\,{\lambda_n}^{\frac{1}{\alpha}-1}$, but *only* for those λ_n satisfying $|\arg(\lambda_n)| < \alpha\pi$);
- any such Mittag-Leffler function has a representation with a pole and a cut on $\mathcal{C} = \mathbb{R}^-$, with a weight which can be computed exactly when $s_n \in \mathbb{C}\backslash\mathbb{R}^-$:

$$\mu_{\alpha,\lambda_n}(\xi) = \frac{\sin(\alpha\pi)}{\pi}\,\frac{\xi^\alpha}{\xi^{2\alpha} - 2\lambda_n\cos(\alpha\pi)\xi^\alpha + {\lambda_n}^2}\,. \tag{21}$$

This is the reason why, at least for simulation purposes, the distinction between commensurate and uncommensurate orders proves a bit artificial.

3.2.3.2 Uncommensurate orders Now, following [3, § 2.3] and[1], for both cases, the following decomposition can be written down for system H_5:

$$h_5(t) = \sum_{k=1}^{K} \sum_{l=1}^{L_k} r_{k,l} \frac{1}{l!} t^{l-1} e^{s_k t} + \int_0^\infty \mu_5(\xi)\, e^{-\xi t}, \qquad \text{for } t > 0. \tag{22}$$

The following remarks apply to the previous decomposition:

- there is only a *finite* number of poles, as proved in [6,14];
- we have an *analytical* knowledge of μ_5, namely (see [3,2]):

$$\mu_5(\xi) = \frac{1}{\pi} \frac{\sum_{k=0}^{p} \sum_{l=0}^{q} a_k b_l \sin((\alpha_k - \beta_l)\pi)\, \xi^{\alpha_k+\beta_l}}{\sum_{k=0}^{p} a_k^2\, \xi^{2\alpha_k} + \sum_{0\le k<l\le p} 2a_k a_l \cos((\alpha_k - \alpha_l)\pi)\, \xi^{\alpha_k+\alpha_l}}\,; \tag{23}$$

- Still, the case of poles on the cut $\mathbb{R}^-$ is difficult, but it can be put in a somewhat larger framework, involving measures or distributions: in this case, the integral term in (22) is to be understood in a generalized sense (see e.g. [20, pp 71–73]). Yet, there is another strategy of representation, which consists in moving the cut between the same branching points ($s = 0$ and $s = -\infty$), so as to avoid the singularities, see e.g. [19].

3.2.4 Diffusive systems

Choosing $\mathcal{C} = \mathbb{R}^-$ and $\gamma = -\xi$ leads to $\mu_6(\xi) = \frac{\cos(\sqrt{\xi})}{\pi\sqrt{\xi}}$, which fulfills (15).

But H_7 must be realized with an extension: $H_7(0) = 1$ and $\breve{\mu}_7 = \frac{\sin(\sqrt{\xi})}{\pi\xi}$; thus, $\breve{\mu}_7$ now fulfills (15).

3.2.5 More complex systems

For H_8, we now have *two* finite branching points, thus many cuts can be proposed, we will only consider the two lines parallel to $\mathbb{R}^-$ stemming from $\pm i$: $\gamma^{\pm}(\xi) = \pm i - \xi$. Following [3, § 3.3], we get:

$$\mu_8^{\pm}(\xi) = \frac{1}{\pi\sqrt{\xi}} \frac{1}{\sqrt{\pm 2i - \xi}}\,, \tag{24}$$

with $\sqrt{s}$ uniquely defined for $s \in \mathbb{C}\backslash\mathbb{R}^-$ as the analytic continuation of $\sqrt{x}$ for $x \in \mathbb{R}^+$. Once again, (15) is fulfilled.

For H_9 and H_{10}, also with *three* finite branching points (0, s_1 and $\overline{s_1}$ with $\Re e(s_1) < 0$), two different cuts will be investigated: either three horizontal

cuts parallel to $\mathbb{R}^-$ ($\mathcal{C} = \mathbb{R}^- \cup \left(s_1 + \mathbb{R}^-\right) \cup \left(\overline{s_1} + \mathbb{R}^-\right)$), or a cross-cut made of the segment between the two branching points and the cut on $\mathbb{R}^-$ ($\mathcal{C} = \mathbb{R}^- \cup [s_1, \overline{s_1}]$): more details can be found in [16].

4 Finite-dimensional approximation and simulation of poles and cut-representation models

In this section, we propose to approximate stable realizations of fractional systems and irrational tranfer functions ((1)-(10)) with finite order differential systems, by picking up a finite subset of points which belong to the cut $\mathcal{C}$ and the set of poles $\mathcal{P}$ of the original system. Two methods are described and the corresponding numerical results are compared in both the frequency and the time domain.

4.1 Approximation by interpolation of the state ϕ

A first method consists in approximating $\phi(\gamma, t)$, $\gamma \in \mathcal{C}$ by

$$\widetilde{\phi}(\gamma, t) = \sum_{m=1}^{M} \phi(\gamma, t)\, \Lambda_m(\gamma), \tag{25}$$

where $\{\Lambda_m\}_{1 \le m \le M}$ defines *continuous piecewise linear interpolating functions* which are non zero on the piece $]\gamma_{m-1}, \gamma_{m+1}[_{\mathcal{C}}$ of the cut $\mathcal{C}$ and such that $\Lambda_m(\gamma_m) = 1$; $(\gamma_m)_{0 \le m \le M_{\mathcal{C}}}$ are sorted with respect to the oriented cut $\mathcal{C}$. Convergence results can be proven, e.g. see [20] for the purely diffusive case $\gamma = -\xi \in \mathbb{R}^-$.

The realization (13)-(14) yields the first-order linear system of dimension M

$$\begin{aligned} \partial_t \widetilde{\phi}_m(t) &= \gamma_m\, \widetilde{\phi}_m(t) + u(t),\ 1 \le m \le M, \\ y(t) &= \sum_{m=1}^{M} \widetilde{\mu}_m\, \widetilde{\phi}_m(t) \end{aligned} \tag{26}$$

with

$$\widetilde{\mu}_m = \int_{[\gamma_{m-1}, \gamma_{m+1}]_{\mathcal{C}}} \mu(\gamma) \Lambda_m(\gamma) \mathrm{d}\gamma,\ 1 \le m \le M. \tag{27}$$

Contribution of poles $\gamma \in \mathcal{P}$ can be performed in the same way with standard finite-order systems which are not detailed here.

4.2 Remark on approximations preserving the hermitian symmetry property

For the case of transfer funtions with an hermitian symmetry, the set $(\gamma_m)_{1\leq m\leq M}$ can be described by $\underline{-\xi} = (-\xi_j)_{1\leq j\leq J}$, $\xi_j > 0$ for poles γ lying on $\mathbb{R}^-$ and by the complex conjugate pair $\underline{\gamma} = (\gamma_k)_{1\leq k\leq K}$ and $\underline{(\overline{\gamma})}$ with $\gamma_k = -\xi'_k + i\omega'_k$, $\xi'_k > 0$, and $\omega'_k > 0$ otherwise. The approximation of $\widetilde{(11)}$ of dimension $M = J + 2K$ can be rewritten

$$\widetilde{H_{\underline{\mu}}}(s) = \sum_{j=0}^{J} \frac{\mu_j}{s+\xi_j} + \sum_{k=0}^{K} \left[\mu_k^R \left(\frac{1}{s-\gamma_k} + \frac{1}{s-\overline{\gamma_k}} \right) + \mu_k^I \left(\frac{i}{s-\gamma_k} + \frac{-i}{s-\overline{\gamma_k}} \right) \right], \quad (28)$$

where $\underline{\mu}$ denotes the vector $\underline{\mu}$, $(\mu_1, \ldots \mu_J, \mu_1^R, \ldots, \mu_K^R, \mu_1^I, \ldots, \mu_K^I)^t \in \mathbb{R}^{J+2K}$, μ_j and $\mu'_k = \mu_k^R + i\mu_k^I$ are the associated weights. Requiring real values for $\underline{\mu}$ ensures hermitian symmetry.

4.3 Approximation by optimization of a criterion

The second method consists in a least-square regularized optimization of the weigths $\underline{\mu}$, by minimizing an appropriate distance between an exact transfer function $H(i\omega)$ and its approximation $\widetilde{H_{\underline{\mu}}}(i\omega)$ in the frequency domain, see e.g.[13,19]. One interest is that the distance can be adapted to optimize some performances.

The criterion to be optimized is

$$\mathcal{C}(\underline{\mu}) = \int_{\mathbb{R}^+} \left| \left(\widetilde{H_{\underline{\mu}}}(i\omega) - H(i\omega) \right) w_H(\omega) \right|^2 M(\mathrm{d}\omega) + \sum_{j=1}^{J} \epsilon_j (\mu_j)^2 + \sum_{k=1}^{K} \epsilon'_k ((\mu_k^R)^2 + (\mu_k^I)^2). \quad (29)$$

The parameters $\epsilon_j \geq 0$ are *regularizing parameters* for the purely diffusive part, and $\epsilon'_k \geq 0$ for the damped oscillating part. They allow to keep the problem well-conditionned when the size $J+2K$ of $\underline{\mu}$ increases. The *measure* M and the *weightening* w_H are chosen according to performances to be optimized.

For instance, *audio performances* are well adapted to H_{10} which can be used for sound processing. Corresponding mesures and weightenings can be obtained as follows:

(i) Frequencies are perceived from 20 Hz to 20 kHz on a *logarithmic scale*. We

choose

$$M(\mathrm{d}\omega) = \mathbf{1}_{\omega_-<\omega<\omega_+}(\omega)\ \ \mathrm{d}\ln\omega = \mathbf{1}_{\omega_-<\omega<\omega_+}(\omega)\,\frac{\mathrm{d}\omega}{\omega}. \tag{30}$$

(ii) The perception of *intensity* is also logarithmic so that we consider the *relative error* $|\widetilde{H_{\underline{\mu}}}(i\omega)-H(i\omega)|/|H(i\omega)|$ rather than the absolute error $|\widetilde{H_{\underline{\mu}}}(i\omega)-H(i\omega)|$. This yields the weightening $w_H(\omega) = 1/|H(i\omega)|$.

(iii) A precise modelling is sufficient for the typical "audio dynamics" of 80 dB. The previous weightening $w_H(\omega)$ can then be revised taking

$$w_H(i\omega) = 1/\mathrm{Sat}_{H,T_r}(i\omega). \tag{31}$$

The saturation function with treshold T_r is defined by $\mathrm{Sat}_{H,T_r}(i\omega)$ equals T_H , T_r $\sup_{\omega_-<\omega<\omega_+}|H(i\omega)|$ if $|H(i\omega)| < T_H$, and equals $|H(i\omega)|$ otherwise. This weightening is finite even for transfer functions with zeros. Note that 80 dB corresponds to $T_r = 10^{-4}$.

(iv) In the case of an extension by derivation $\breve{H}$, e.g. $\breve{H}_3$, we need an optimization for H through that of $\breve{H}$. Hence, the weightening to apply to $\breve{H}$ is then that of H with a compensation of the derivation s in (17), that is,

$$\breve{w}_H(i\omega) = \omega/\mathrm{Sat}_{H,T_r}(i\omega). \tag{32}$$

Note that the saturation function is parameterized by H and not $\breve{H}$, but that the weightening $\breve{w}_H$ will be applied on $\breve{H}$ in (29).

The weightening (i-ii) is also well-adapted to the Bode diagram scales. We will use essentially this weightening which is noted $W_{log,rel}$ (logarithmic scale for frequencies and relative error) and sometimes the *uniform weightening* $W_{unif} = 1$ with the Lebesgue measure $\mathrm{d}\omega$.

For numerical computations, the criterion is computed for a finite set of angular frequencies $\big(\omega_n\big)$, $1 \le n \le N+1$ increasing from $\omega_1 = \omega_-$ to $\omega_{N+1} = \omega_+$. It is approximated by

$$\begin{aligned}\mathcal{C}(\underline{\mu}) = &\sum_{n=1}^{N}\Big|\Big(\widetilde{H_{\underline{\mu}}}(i\omega_n) - H(i\omega_n)\Big)w_H(\omega_n)\Big|^2\Big[\ln\omega_{n+1} - \ln\omega_n\Big]\\ &+\sum_{j=1}^{J}\epsilon_j(\mu_j)^2 + \sum_{k=1}^{K}\epsilon'_k((\mu_k^R)^2 + (\mu_k^I)^2).\end{aligned} \tag{33}$$

It takes the equivalent matrix formulation

$$\mathcal{C}(\underline{\mu}) = (\underline{M}\underline{\mu} - \underline{H})^*\underline{W}^*\underline{W}(\underline{M}\underline{\mu} - \underline{H}) + \underline{\mu}^t\underline{E}\underline{\mu}, \tag{34}$$

where $\underline{M}^*$, $\overline{\underline{M}}^t$ denotes the transpose conjugate matrix of $\underline{M}$. The matrix $\underline{M}$ is defined by $M_{n,m} = [i\omega_n + \xi_m]^{-1}$ for $1 \le m \le J$, by $M_{n,m} = \frac{1}{i\omega_n - \gamma_{m-J}} +$

$\frac{1}{i\omega_n-\overline{\gamma_{m-J}}}$ for $J+1 \le m \le J+K$, and by $M_{n,m} = \frac{i}{i\omega_n-\gamma_{m-(J+K)}} + \frac{i}{i\omega_n-\overline{\gamma_{m-(J+K)}}}$ for $J+K+1 \le m \le J+2K$. The vector $\underline{H}$ is the columun vector $\big(H(i\omega_n)\big)_{1\le n\le N}$. The weightening matrix $\underline{W}$ is real positive diagonal and defined by $W_{n,n} = w_H(\omega_n)\sqrt{\ln\omega_{n+1} - \ln\omega_n}$ for $1 \le n \le N$ (recall that $\omega_1 = \omega_-$ and $\omega_{N+1} = \omega_+$). The regularizing matrix $\underline{E}$ is real non negative diagonal and defined by $E_{m,m} = \epsilon_m$ for $1 \le m \le J$ and by $E_{m,m} = E_{K+m,K+m} = \epsilon'_m$ for $J+1 \le m \le J+K$.

Solving this least-square problem with the constraint that $\underline{\mu}$ is real valued yields

$$\underline{\mu} = [\Re\mathrm{e}(\underline{M}^*\,\underline{W}^*\,\underline{W}\underline{M}) + \underline{E}]^{-1}\ \Re\mathrm{e}(\underline{M}^*\,\underline{W}^*\,\underline{W}\underline{H}). \tag{35}$$

This result is obtained by decomposing the complex values as $x+iy$, solving the problem and recomposing the result into the compact form (35).

4.4 Results in the frequency domain

Plots of $\mu(\gamma)$ and results for both approximations (27) and (35) are presented in Fig.1-Fig.6 for H_1 to H_4, H_6, H_8 and H_{10}. A general remark is that the approximation by optimization does not require to compute $\mu(\gamma)$ and, for a given pole placement $(\gamma_m)_{1\le m\le M}$, it yields results much better than those obtained by interpolation. Nevertheless, the analysis of $\mu(\gamma)$ is required to check the well-posedness condition (15) and is usefull to build relevant pole placements $(\gamma_m)_{1\le m\le M}$. This last point is illustrated for H_6 in Fig.4.

4.5 Time-domain simulations

The finite-dimensional realizations of the approximated transfer functions are

$$\partial_t\phi_j(t) = -\xi_j\,\phi_j(t) + u(t), \qquad 1 \le j \le J, \tag{36}$$

$$\partial_t\phi'_k(t) = (-\xi'_k + i\omega'_k)\,\phi'_k(t) + u(t), \qquad 1 \le k \le K, \tag{37}$$

$$\widetilde{y}(t) = \sum_{j=1}^{J} \mu_j\phi_j(t) + 2\Re\mathrm{e}\sum_{k=1}^{K} \mu'_k\phi'_k(t), \tag{38}$$

$$\begin{aligned}\widetilde{z}(t) = &\sum_{j=1}^{J}(-\xi_j\breve{\mu}_j)\phi_j(t) + 2\Re\mathrm{e}\sum_{k=1}^{K}(-\xi'_k + i\omega'_k)\breve{\mu}'_k\phi_k(t)\\ &+\Big[H(0)+\sum_{j=1}^{J}\breve{\mu}_j + 2\Re\mathrm{e}\sum_{k=1}^{K}\breve{\mu}'_k\Big]u(t),\end{aligned} \tag{39}$$

where $\widetilde{y}(t)$ stands for the output of a standard representation while $\widetilde{z}(t)$ stands for the output of an extension by derivation (17).

Approximating $u(t)$ by its *sample and hold version*, that is $u(t) \approx u(t_n)$ for $t_n \leq t < t_{n+1}$, equations (36)-(39) become, in the discrete-time domain,

$$\phi_j(t_n) = \alpha_j\, \phi_j(t_{n-1}) + \frac{\alpha_j - 1}{-\xi_j} u(t_{n-1}) \tag{40}$$

$$\phi'_k(t_n) = \alpha'_k\, \phi'_k(t_{n-1}) + \frac{\alpha'_k - 1}{-\xi'_k + i\omega'_k} u(t_{n-1}) \tag{41}$$

$$\widetilde{y}(t_n) = \sum_{j=1}^{J} \mu_j \phi_j(t_n) + 2\Re\mathrm{e} \sum_{k=1}^{K} \mu'_k \phi'_k(t_n), \tag{42}$$

$$\begin{aligned} \widetilde{z}(t_n) = &\sum_{j=1}^{J} (-\xi_j \breve{\mu}_j) \phi_j(t_n) + 2\Re\mathrm{e} \sum_{k=1}^{K} (-\xi'_k + i\omega'_k) \breve{\mu}'_k \phi'_k(t_n) \\ &+ \Big[H(0) + \sum_{j=1}^{J} \breve{\mu}_j + 2\Re\mathrm{e} \sum_{k=1}^{K} \mu'_k \Big] u(t_n). \end{aligned} \tag{43}$$

where $t_n = n\, T_s$, T_s is the sampling period, $\alpha_j = \mathrm{e}^{-\xi_j T_s}$ and $\alpha'_k = \mathrm{e}^{(-\xi'_k + i\omega'_k) T_s}$.

The impulse responses $h_4(t_n)$, $h_6(t_n)$, $h_8(t_n)$ and $h_{10}(t_n)$ are simulated thanks to these recursive equations for both the approximations by interpolation and by optimization. The results for approximations by optimization are still better than those obtained by interpolation. They are presented in Fig.3-Fig.6.

5 Perspectives

Further works are in view: for the final version of the present paper, a comparison with Mittag-Leffler functions will be provided for example H_4; also more worked out examples will be presented, such as H_5, H_7 and H_9 with both horizontal cuts and cross-cuts.

Some interesting questions remain still open. Firstly, the choice of the cut between fixed branching points in the left-half complex plane can be made on different criteria, but it is not easy to know *a priori* which representation fits best. Secondly, once a cut has been chosen, what is the optimal pole placement on it, in order to reduce the infinite-dimensional system to a finite-order approximation (more suitable for time-domain simulation)? Both these questions are quite involved from a theoretical point of view; nevertheless, they must be taken into consideration, for they can have serious numerical consequences for the finite-dimensional approximation of our fractional systems.

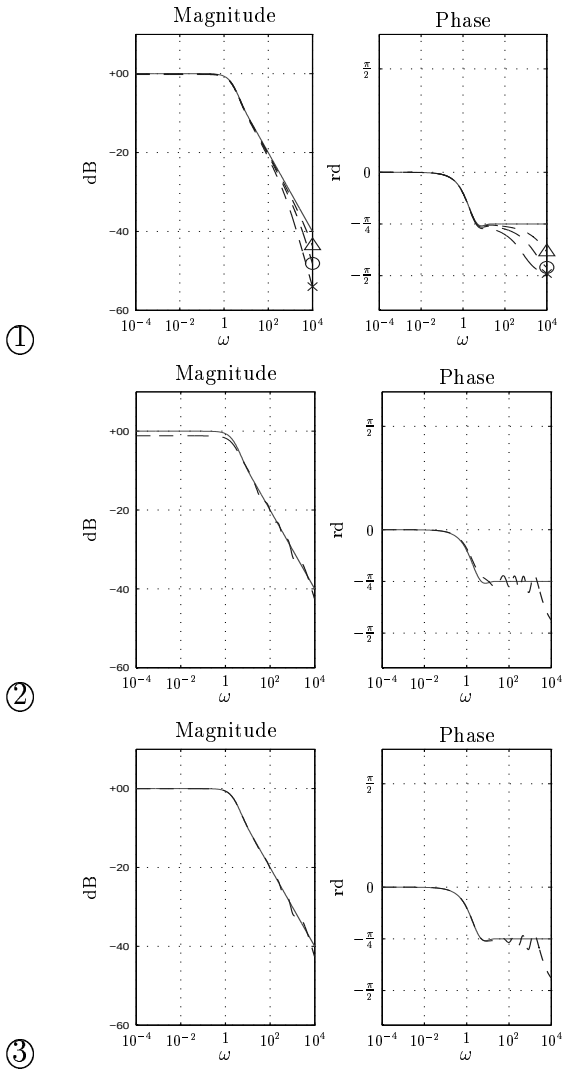

Fig. 1. Bode diagrams for transfer function H_1: ① exact (-), truncated series with the N first poles, N=10 ($\times$), N=20 (o) and $N = 40$ ($\triangle$); ② exact (-) and optimized (- -) with $N = 10$ and $W = W_{unif}$; ③ exact (-) and optimized (- -) with $N = 10$ and $W = W_{log,rel}$.

Finally, it will be of utmost interest to enlarge the class of irrational tranfer functions by allowing for *delay* systems to be present: so far, they have not been taken into account in our framework; even if some theoretical results are available, this will be a wide open direction of research concerning representation and simulation of such systems.

6 Conclusion

A powerful and very flexible method of simulation of *fractional* systems has been presented: it uses a simple optimization procedure with parameters which

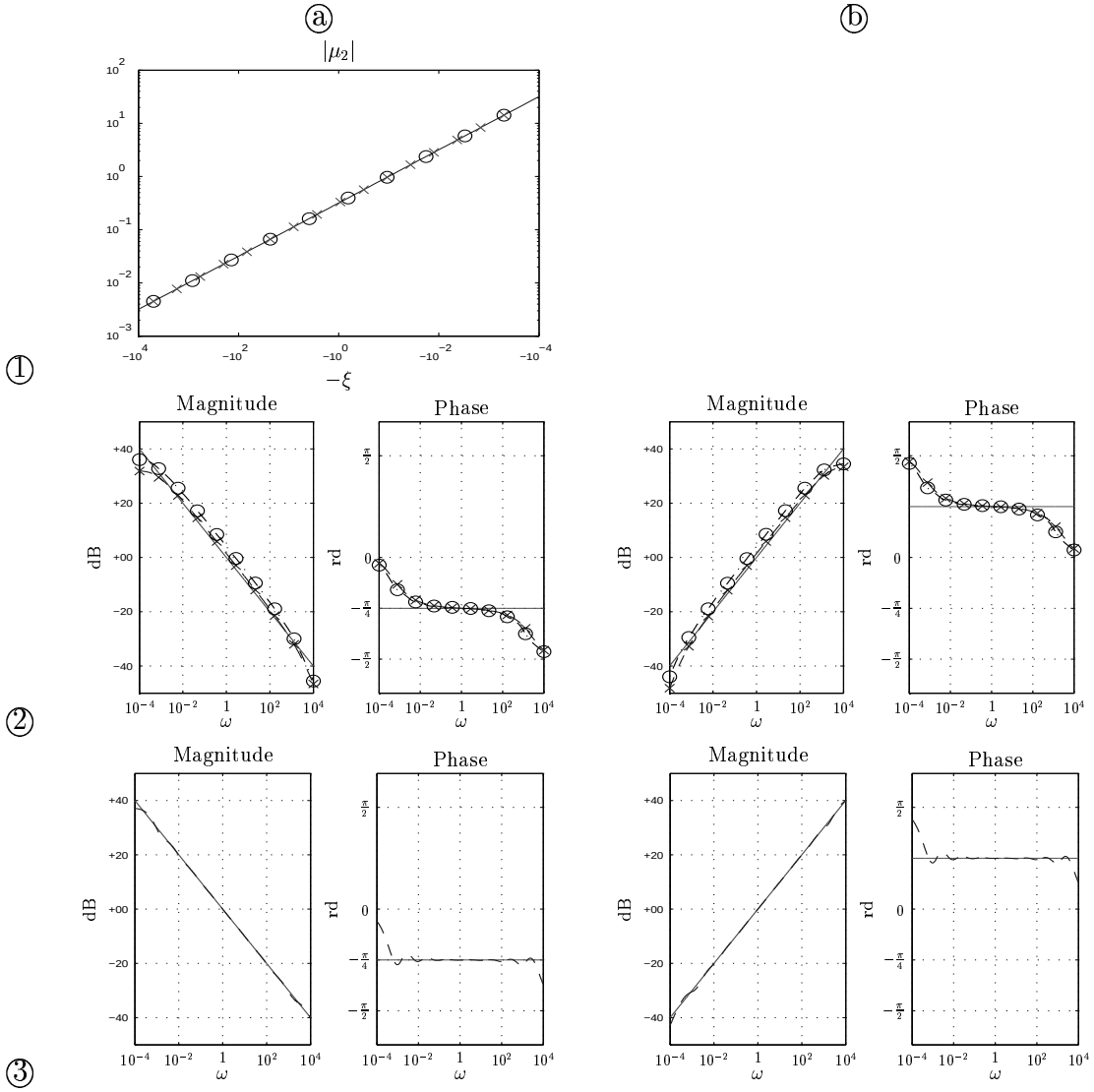

Fig. 2. Weight $\mu_2(\xi) = \breve{\mu}_3(\xi)$ for $\beta = 1 - \alpha = 1/2$ (1,a) and two logarithmic pole placements with $N = 10$ (o), $N = 16$ ($\times$) between $\xi_{min} = 5.10^{-4}$ and $\xi_{max} = 5.10^{3}$. The corresponding bode diagrams are in column ⓐ for H_2 and in ⓑ for H_3. The line ② gives the exact Bode diagrams (-), and the result of interpolations ($o, \times$). The line ③ gives the exact Bode diagrams (-), and the result of optimization (- -) for the case $N = 10$ with $W = W_{log,rel}$.

are meaningful from a signal processing point of view, and it enables a low cost simulation, both in the frequency domain and in the time domain. From a a theoretical point of view, this method is based on a *representation with poles and cuts*, which generalizes the so-called diffusive representations. A family of ten such systems, among which fractional differential systems, is presented throughout the paper, which clearly illustrates the generality, the flexibility and the power of this method.

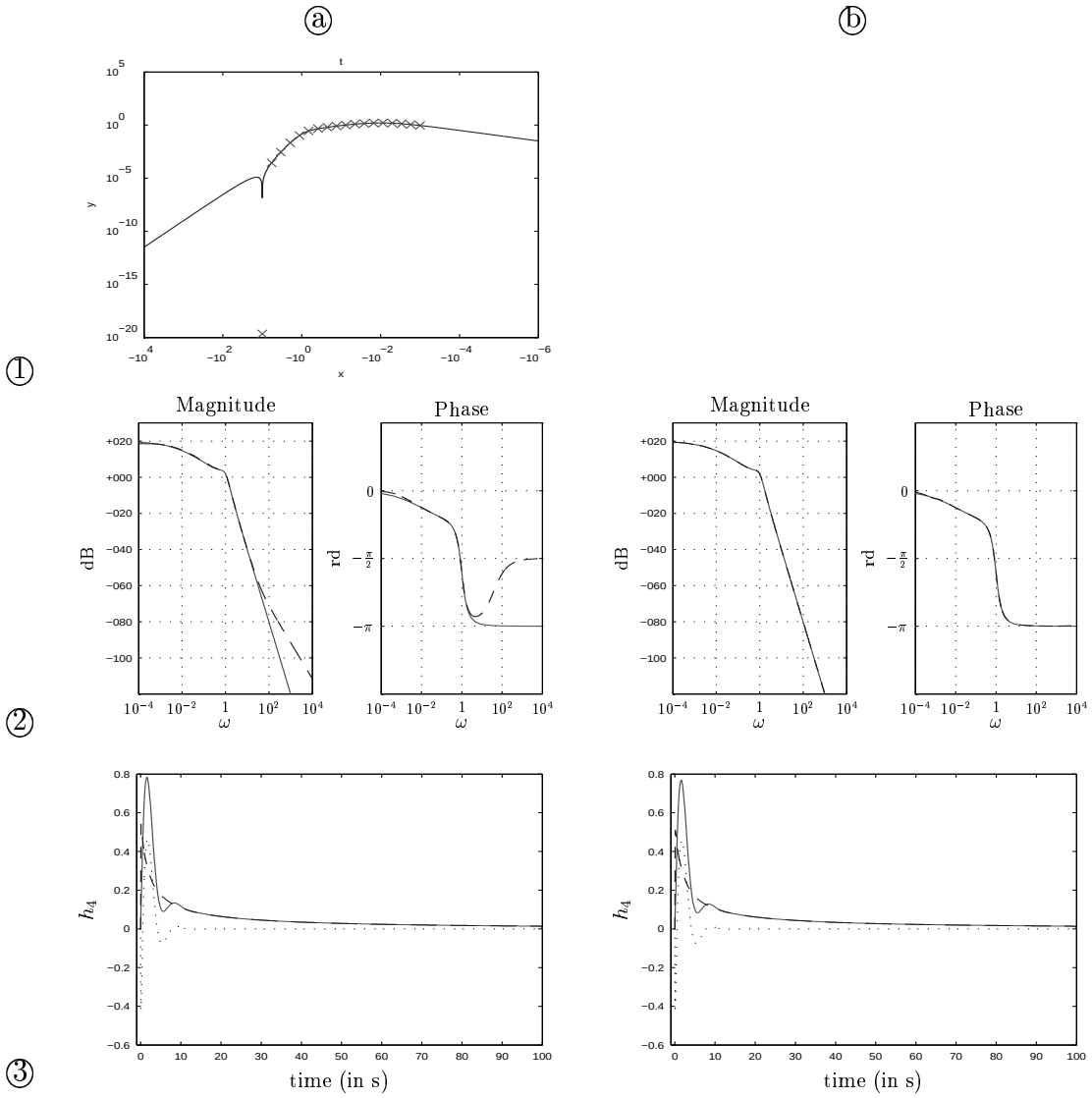

Fig. 3. Weight $\mu_4(\xi)$ with [20] $\alpha = 1/2$, $Q(\sigma) = 1$ and $P(\sigma) = \sigma^4 + 0.1\sigma^3 + \sigma + 0.1$ (1,a) and logarithmic pole placement ($\times$) with $N = 18$ between $\xi_{min} = 1.10^{-3}$ and $\xi_{max} = 10$. The column ⓐ corresponds to exact (-) and interpolated (- -) results, and the column ⓑ to exact (-) and optimized (- -) results with $W = W_{log,rel}$. The line ② gives Bode diagrams. In line ③, discrete time simulations are presented for $f_s = 10^4/\pi$: $h_4(t)$ are in solid lines (-), the diffusive part in dashed lines (- -) and the second order oscillatory part in dotted lines (:).

References

[1] J. Audounet, D. Matignon, G. Montseny, Opérateurs différentiels fractionnaires, opérateurs pseudo-différentiels, représentations diffusives, Tech. Report 99501, LAAS, 1999.

[2] G. Dauphin, D. Heleschewitz, D. Matignon, Extended diffusive representations and application to non-standard oscillators, in: Proceedings of the Mathematical

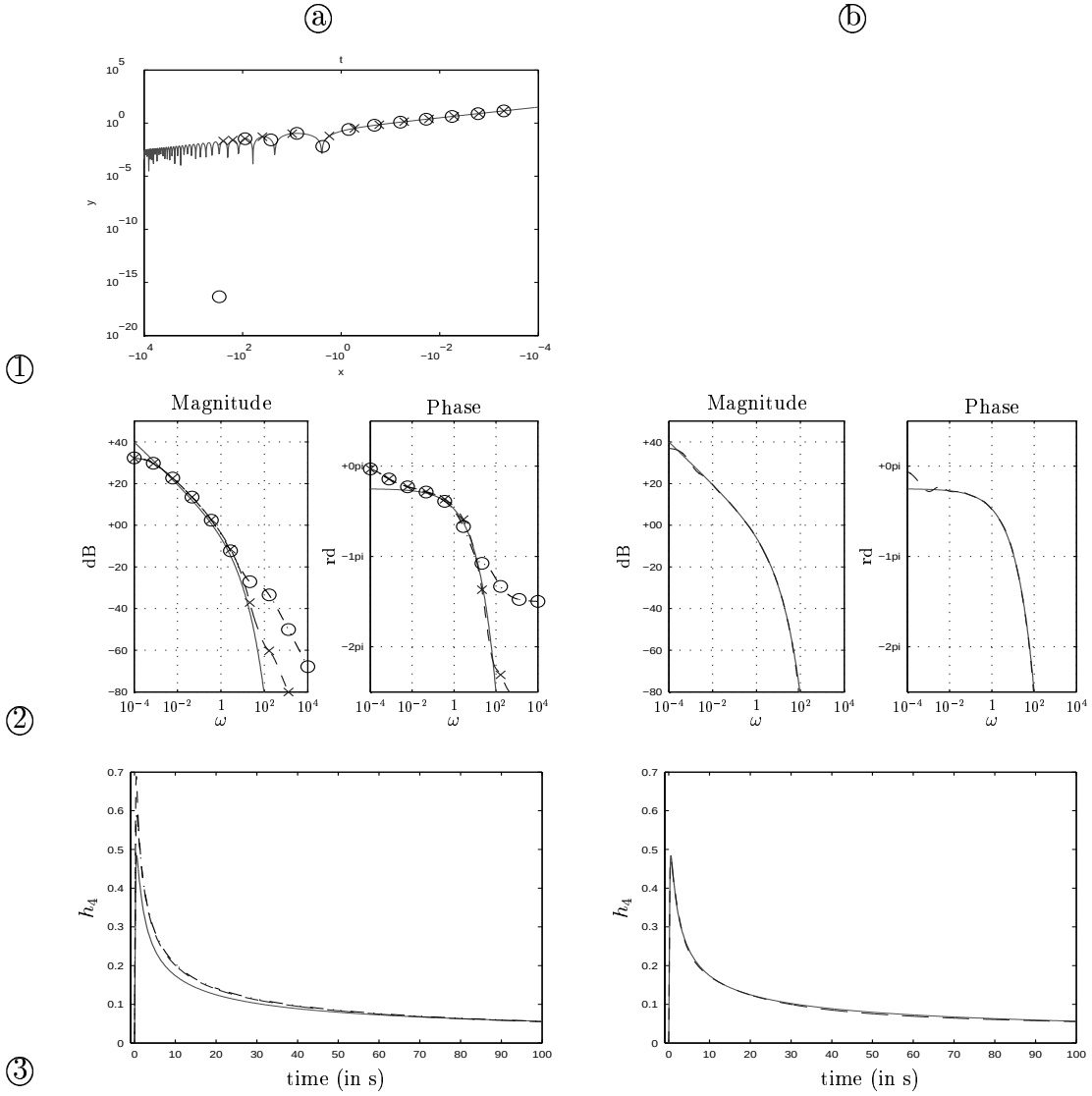

Fig. 4. Weight $\mu_6(\xi)$ and two pole placements with $N = 12$ between $\xi_{min} = 5.10^{-4}$ and $\xi_{max} = 3.10^2$: one is purely logarithmic (o), whereas the second one ($\times$ is modified to match with some maxima of $|\mu_6|$. The column ⓐ corresponds to exact (-) and interpolated (o,$\times$) results, and the column ⓑ to exact (-) and optimized (- -) results with $W = W_{log,rel}$ and the placement $\times$. The line ② gives Bode diagrams. In line ③, discrete time simulations are presented for $f_s = 10^4/\pi$: the exact kernel $h_6(t)$ is in solid lines (-); the kernels computed for the interpolations (o,$\times$) are very similar and both represented with the dashed lines in (3,a); in (3,b), the exact and optimized impulse responses superimpose.

Theory of Networks and Systems symposium, MTNS, Perpignan, France, 2000, 10 p., (invited session).

[3] D. Matignon, Stability properties for generalized fractional differential systems, ESAIM: Proceedings 5 (1998) 145–158,
URL: `http://www.edpsciences.org/articlesproc/Vol.5/`.

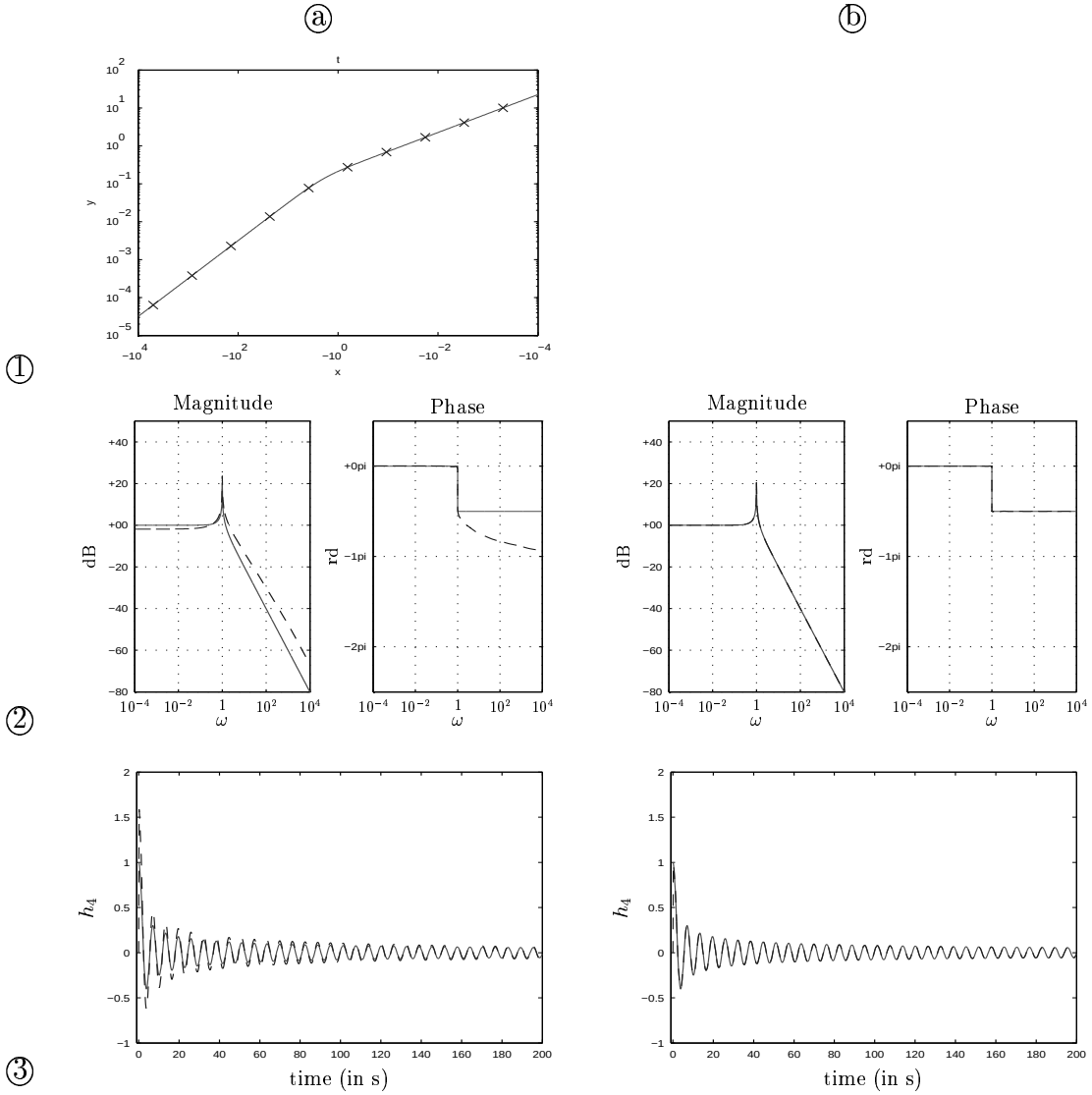

Fig. 5. Weight $\mu_8(\xi)$ for a logarithmic pole placement ($\times$) with $N = 10$ between $\xi_{min} = 5.10^{-4}$ and $\xi_{max} = 5.10^{3}$. The column ⓐ corresponds to exact (-) and interpolated (- -) results, and the column ⓑ to exact (-) and optimized (- -) results with $W = W_{log,rel}$. The line ② gives Bode diagrams. In line ③, discrete time simulations are presented for $f_s = 10^4/\pi$: the exact $h_8(t)$ is in solid lines (-), the approximated kernels are in dashed lines (- -).

[4] D. Matignon, H. Zwart, Diffusive systems as well-posed linear systems, Systems & Control Letters. Submitted.

[5] O. J. Staffans, Well-posedness and stabilizability of a viscoelastic equation in energy space, Trans. Amer. Math. Soc. 345 (2) (1994) 527–575.

[6] C. Bonnet, J. R. Partington, Coprime factorizations and stability of fractional differential systems, Systems & Control Letters 41 (2000) 167–174.

[7] K. S. Miller, B. Ross, An introduction to the fractional calculus and fractional differential equations, John Wiley & Sons, 1993.

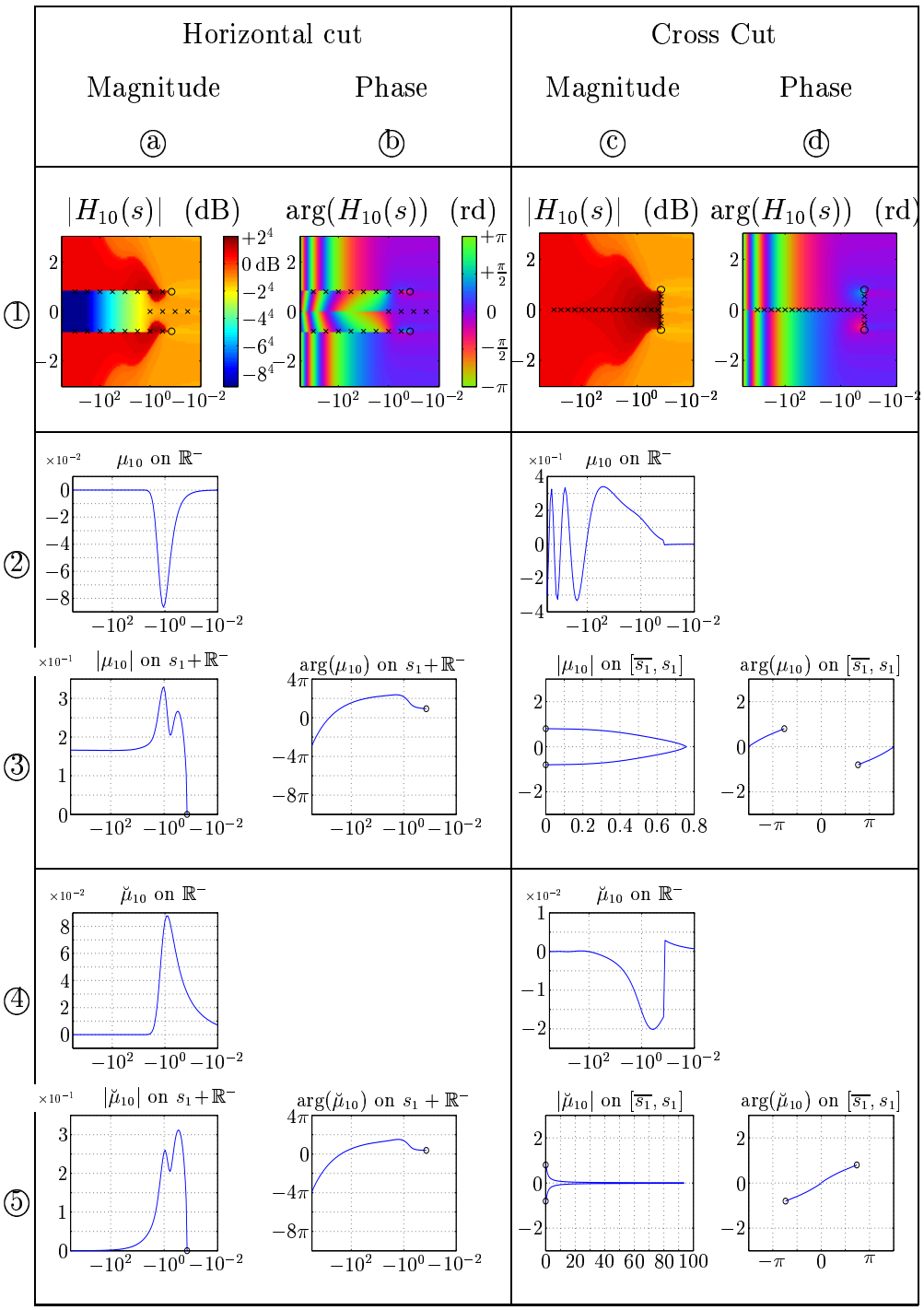

Fig. 6. Magnitude and phase of H_{10}, $s \in \mathbb{C}_0^-$ are represented in ① for horizontal cuts (a,b) and cross-cut (c,d). The corresponding (real-valued) μ_{10} computed on $\mathbb{R}^-$ are in ②a,c. The corresponding (complex-valued) are computed on $s_1 + \mathbb{R}^-$ (③a:modulus, ③b:phase) and on $[\overline{s_1}, s_1]$ (③c:magnitude, ③d:phase), respectively. The X-axis of ①, ② and ③a,b correspond to $-\xi = \Re\mathrm{e}(s) < 0$ on a log-scale, and the Y-Axis of ①, ③c,d to $\omega = \Im\mathrm{m}(s)$ on a linear scale. Circles o represent branching points and crosses $\times$ the pole placement for the approximation. The weights μ in ②c and ③a do not decrease when $-\xi \to -\infty$ so that the well-posedness condition (15) is not satisfied. This problem disappears in ④, ⑤ for the extension by derivation $\breve{\mu}_{10}$ computed from $\breve{H}_{10}(s)$.

[8] H. Zwart, Transfer functions for infinite-dimensional systems, Systems & Control Letters 52 (3-4) (2004) 247–255.

[9] R. F. Curtain, H. J. Zwart, An introduction to infinite–dimensional linear systems theory, Vol. 21 of Texts in Applied Mathematics, Springer Verlag, 1995.

[10] D. Matignon, G. Montseny (Eds.), Fractional Differential Systems: models, methods and applications, Vol. 5 of ESAIM: Proceedings, SMAI, URL: `http://www.edpsciences.org/articlesproc/Vol.5/`, 1998.

[11] A. Carpinteri, F. Mainardi (Eds.), Fractals and fractional calculus in continuum mechanics, no. 378 in CISM courses and lectures, Springer Verlag, 1997.

[12] D. G. Duffy, Transform methods for solving partial differential equations, CRC Press, 1994.

[13] G. Garcia, J. Bernussou, Identification of the dynamics of a lead acid battery by a diffusive model, ESAIM: Proceedings 5 (1998) 87–98, URL: `http://www.edpsciences.org/articlesproc/Vol.5/`.

[14] C. Bonnet, J. R. Partington, Analysis of fractional delay systems of retarded and neutral type, Automatica 38 (7) (2002) 1133–1138.

[15] A. Oustaloup, Systèmes asservis linéaires d'ordre fractionnaire, Série Automatique, Masson, 1983.

[16] T. Hélie, D. Matignon, Diffusive reprentations for the analysis and simulation of flared acoustic pipes with visco-thermal losses, Mathematical Models and Methods in Applied Sciences. Submitted.

[17] H. Haddar, T. Hélie, D. Matignon, A Webster-Lokshin model for waves with viscothermal losses and impedance boundary conditions: strong solutions, in: Proceedings of the sixth international conference on mathematical and numerical aspects of wave propagation phenomena, INRIA, Jyväskylä, Finland, 2003, pp. 66–71.

[18] T. Hélie, D. Matignon, Numerical simulation of acoustic waveguides for Webster-Lokshin model using diffusive representations, in: Proceedings of the sixth international conference on mathematical and numerical aspects of wave propagation phenomena, INRIA, Jyväskylä, Finland, 2003, pp. 72–77.

[19] M. Dunau, Représentations diffusives de seconde espèce : introduction et expérimentation, Master's thesis, DEA d'Automatique, Toulouse (2000).

[20] D. Heleschewitz, Analyse et simulation de systèmes différentiels fractionnaires et pseudo-différentiels linéaires sous représentation diffusive, Ph.D. thesis, ENST, Paris (December 2000).

[21] G. Mittag-Leffler, Sur la représentation analytique d'une branche uniforme d'une fonction monogène, Acta Math. 29 (1904) 101–168.

[22] E. Zwicker, R. Feldtkeller, Psychoacoustique - L'oreille, récepteur d'information, Collection technique et scientifique des télécommunications, Masson, 1981.